Revision of forensics-relevant nuclear data in ^{127}Sb β decay

B. Bucher,* M. S. Snow, E. S. Cárdenas, K. P. Carney, M. R. Finck, J. J. Horkley, M. T. Kinlaw, E. M. May, J. K. Pfeiffer, and J. L. Ward

Nuclear Nonproliferation Division, Idaho National Laboratory, Idaho Falls, Idaho 83415, USA

(Received 5 December 2018; published 14 March 2019)

With a half-life of 3.85(5) d, the fission product ^{127}Sb is potentially useful for the characterization of fallout debris that would be collected for forensic analysis following a hypothetical nuclear event. The β decay of ^{127}Sb has many characteristic γ-ray lines, however, the majority of decay strength is concentrated in the three strongest lines near 686, 473, and 784 keV, based on low-precision spectroscopic measurements from decades ago. In a new measurement of ^{127}Sb β decay, obtained from radiochemical separations of U photofission products, we show that the energies of the 686 and 784 lines are actually shifted lower by 0.8 and 1.1 keV, respectively. Such large discrepancies in the nuclear data inhibit accurate isotopic analyses and have important implications, for example, on the assessment of fission debris that might be collected in the days following a nuclear event. Therefore, a new evaluation of ^{127}Sb β decay and appropriate revisions to the various nuclear databases are warranted. This paper reports a new set of γ-ray energies and relative intensities corresponding to ^{127}Sb decay.

DOI: 10.1103/PhysRevC.99.034314

I. INTRODUCTION

Nuclear forensics is concerned with, among other things, the accurate assessment of fallout that would be collected from the environment in the hours, days, weeks, and months following a nuclear detonation. It is a relatively young field aimed towards the development and refinement of a capability that is important for the peace and security of nations around the world, not only as a deterrent to rogue state actors, but to ensure retribution could be appropriately dealt if needed as to prevent any future hostilities [1] (see Ref. [2] for a broad overview of the field). In support of this effort, our laboratory is evaluating different methods to produce realistic surrogate nuclear fallout debris for testing collection and radiochemical analysis methods [3]. This is needed as real samples containing short-lived fission products in appropriate abundances have not been available since the ban on nuclear testing. The long term goal of this project is to have a surrogate debris containing short-lived fission product radionuclides relevant for supporting exercises involving chemistry and evaluation of simulated nuclear fallout.

From a more fundamental point of view, the basic idea of reconstructing past nuclear events based on present physical observations has been common to many application across nuclear science. A few examples include the evaluation of reactor operating conditions from analysis of fuel rods [4], the determination of radiological doses in the atomic bomb survivors of Hiroshima [5], or even in defining the cosmological processes influencing the chemical makeup of our galaxy [6]. The nuclear fallout problem is similar but has the added complication of chemical fractionation that must also be sorted out [7,8]. Nevertheless, an accurate reconstruction of the event in question relies heavily on the availability of quality nuclear data. For this purpose, the most relevant nuclear data pertains to the production mechanisms (e.g., neutron capture or fission) and radioactive decay (α and β) of the involved isotopes. An important component of the forensic evidence is obtained from γ-ray spectroscopy of collected fallout debris. For this purpose, the most critical nuclear data are γ-ray energies and intensities produced in β decay, largely for neutron-rich fission isotopes having lifetimes in the hours to months timescale.

The fission product ^{127}Sb is a particularly good example of a forensics-useful isotope. It is relatively strongly produced from neutron-induced fission of uranium and plutonium isotopes with significant variation depending on the specific isotopes and neutron energies involved [9,10]. With a half-life of 3.85 d, it can be prominently observed in the earliest possible debris collections and measurements. Its decay branching is mainly concentrated through only a few γ-ray lines with intermediate-range energies where the intense Compton background characteristic of fission spectra is not so strong and where there are less overlapping γ-ray lines from the many other fission isotopes present. Moreover, the γ-ray energies are still low enough to have a fairly good photopeak detection efficiency in high-resolution germanium detectors which helps allow for a precise determination of its activity within a given sample. These characteristics make ^{127}Sb an ideal candidate for incorporation into surrogate debris to make the isotopic mixture of the surrogate more complete. As such our laboratory has begun developing methods to isolate fission produced antimony isotopes. Through the study of various γ-ray spectra recorded from fission samples, it has been noticed that a few of the very strongest ^{127}Sb decay lines seem to have energies that significantly deviate from the evaluated values tabulated in Refs. [11,12]—by as much as 1 keV or more. This paper reports on one of those experiments and provides

*brian.bucher@inl.gov

updated γ-ray energies and intensities corresponding to ^{127}Sb decay. In the following, details regarding the experimental production and radiochemical separation of ^{127}Sb are provided in Sec. II. The collection of γ-ray spectra and analysis procedures are outlined in Sec. III while the subsequent results are discussed in Sec. IV with conclusions provided in Sec. V.

II. EXPERIMENT

The main objective of the present experiment was geared towards the production and chemical purifications of a range of different isotopes relevant to nuclear forensic interests. Therefore, only a fraction of the total experimental resources was dedicated to ^{127}Sb, which, unfortunately, forced tight constraints on the decay measurement time that could be devoted to this isotope, thus limiting the experimental sensitivity. Nevertheless, this and many other neutron-rich, radioactive isotopes were originally produced in large quantities through photofission of uranium. A 118 mg natural uranium target was irradiated with the Idaho Accelerator Center's 44 MeV electron linac [13]. Bremsstrahlung radiation was generated by impinging 26 MeV electrons on a 0.1 inch thick tungsten radiator. Two inches of aluminum were positioned immediately downstream from the tungsten, followed by the uranium target located 2 cm from the end of the aluminum. The integrated electron charge during the 7 h irradiation was 2.5 C and resulted in an estimated 6×10^{12} photofission reactions. Following irradiation, the target cooled for 3 d prior to being shipped to Idaho National Laboratory's Materials and Fuels Complex for chemical processing.

Dissolution of the target began 90 h after the end of irradiation. The uranium foil was placed in a Teflon container, following which 1 mL of concentrated nitric acid was added. The vial was loosely capped and heated on a hotplate at 150 °C for 40 min to completely dissolve. The sample was then diluted to a concentration of 3 M HNO_3 using 18 MΩ deionized water and passed through a tandem UTEVA-Diphonix (Eichrom Industries) column setup, with uranium retained on the UTEVA column and antimony, tin, and indium, along with trace amounts of other fission products, retained on the Diphonix column. The column stack was rinsed with 3 M HNO_3, following which a combined Sb-Sn-In fraction was eluted from the Diphonix column into a 50 mL Corning centrifuge tube using 15 mL of 3 M HCl.

Following separation, the centrifuge tube was placed 10 cm from the front face of a liquid nitrogen cooled coaxial high-purity Ge (HPGe) detector of 12% relative efficiency. A compact Ortec DSPEC jr 2.0 module was used to handle signal processing and data acquisition. Lead bricks were arranged on all sides of the HPGe to suppress background radiation from the environment. The γ-ray detection efficiency as a function of energy (Fig. 1) was determined using a 5 mL solution of calibrated mixed isotope standards purchased from Eckert & Ziegler Isotope Products [14] and placed in a 20 mL Wheaton liquid scintillation (LSC) vial. As a way to quantify and correct for the systematic error introduced from differences between the sample geometries and the calibration geometry, i.e., different volumes and test tube sizes, a solution of ^{140}Ba ($T_{1/2} = 12.75$ d) and its daughter ^{140}La in 3 M HNO_3 was

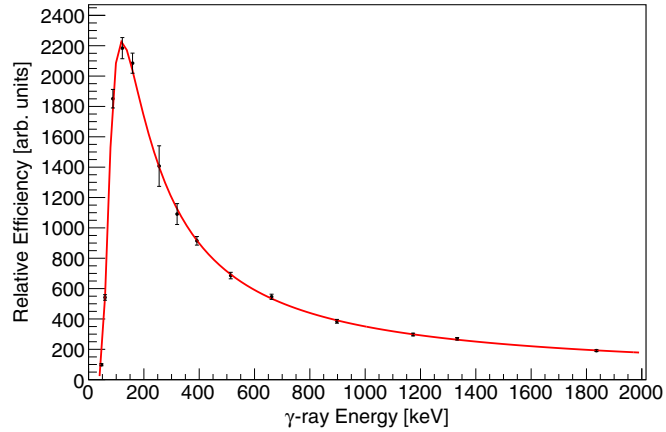

FIG. 1. The HPGe efficiency curve determined from a 5 mL solution of mixed isotope standards.

counted in three different configurations: 1) 29 mL in a centrifuge tube, 2) 1 mL in a LSC vial, and 3) the same 1 mL diluted with water to 5 mL in a LSC vial, the latter matching exactly the calibration geometry.

The separated Sb sample was first counted for 8.7 min (with negligible detector dead time) at 97 h after irradiation. This was done mainly for the purpose of evaluating the chemical separation method in terms of its efficiency for the radioisotopes of interest, i.e., ^{126,127}Sb, as well as to identify any other radioisotopes present in the solution. The latter consisted primarily of ^{125}Sn and ^{115m}In along with trace fractions of ^{99m}Tc, ^{103}Ru, ^{105}Rh, ^{131,132,133}I, and ^{111,112}Ag. Note that the short-lived isotopes ^{115m}In ($T_{1/2} = 4.49$ h), ^{99m}Tc ($T_{1/2} = 6.00$ h), ^{132}I ($T_{1/2} = 2.30$ h), and ^{112}Ag ($T_{1/2} = 3.13$ h) were produced from the decay of their respective longer-lived parents, ^{115}Cd ($T_{1/2} = 53.46$ h), ^{99}Mo ($T_{1/2} = 66.0$ h), ^{132}Te ($T_{1/2} = 76.9$ h), and ^{112}Pd ($T_{1/2} = 21.0$ h), existing in the base solution. The sample was then counted a second time 20 h later for 17.2 min to achieve better statistics for the Sb decays with the added bonus that the shorter-lived contaminants had mostly decayed away or were substantially reduced. Figure 2 shows a comparison of the two spectra, live-time normalized, with the photopeaks identified.

III. ANALYSIS

For the most precise determination of γ-ray energies and intensities, the first count of the Sb sample (hereafter referred to as Sb^1) is not ideal mainly because of the many contaminant lines complicating the spectrum; in particular the short-lived ^{132}I introduces a large number of lines into the spectrum (Fig. 2). In the later measurement (hereafter Sb^2), most of the activity from the shortest-lived isotopes is gone, while the longer count time enables more of the low-intensity ^{127}Sb lines to be observed. Nevertheless, Sb^1 does have an important advantage in that the strong contaminant lines can be used to provide a precise energy calibration, free from systematic error induced by drifting electronics. On the other hand, due to the decay of most contaminants in Sb^2, there are not enough non-Sb lines with ample statistics in the spectrum to

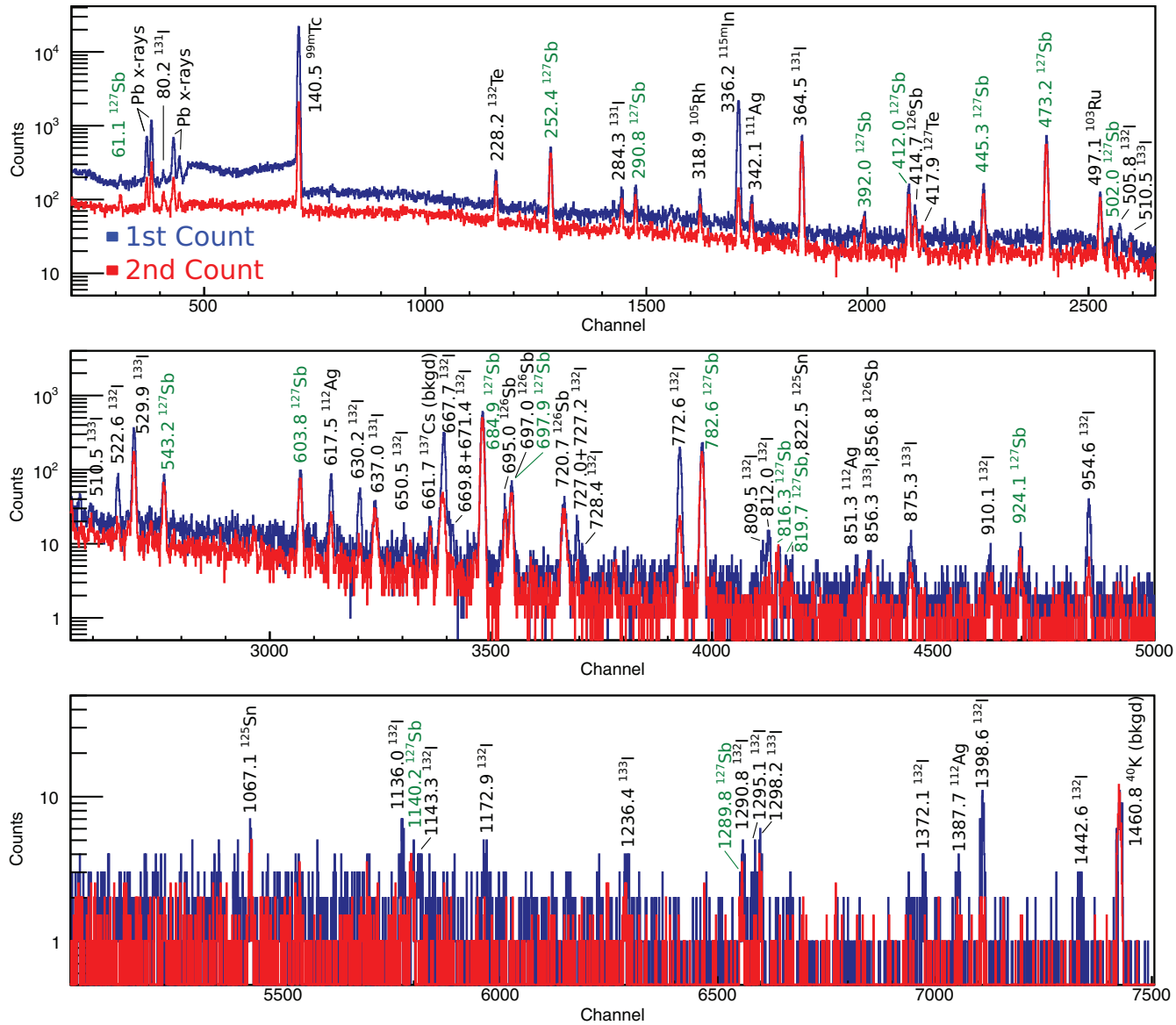

FIG. 2. The two counts of the Sb sample are compared (second count live-time normalized to the first). The second count was recorded 20 h after the first; note the drastic reduction in photopeak intensities for the short-lived isotopes ^{99m}Tc, ^{115m}In, ^{112}Ag, and ^{132}I. The Pb x rays, 662 keV ^{137}Cs line, and 1461 keV ^{40}K line are artifacts of the laboratory environment.

provide such a calibration. Therefore, the energy calibration must be obtained from a separate spectrum. Fortunately, a suitable calibration spectrum was obtained 1.2 h prior using the mixed isotope calibration standard mentioned in Sec. II which contained a range of strong γ-ray lines from 46.5 keV (^{210}Pb) up to 1836.1 keV (^{88}Y). Despite the short time difference between the calibration and Sb^2 measurements, however, a small correction and associated uncertainty was still implemented to properly account for any potential drift between the two spectra. The magnitude and uncertainty of the drift can be estimated by comparing centroids of prominent γ-ray lines in the two Sb spectra. Figure 3 shows the differences in centroids for several lines from various isotopes in the spectra (i.e., ^{127}Sb, ^{131,132,133}I, ^{103}Ru, and ^{112}Ag). The shifts in centroids have no apparent energy dependence as a sloped-fit to the data does not improve the overall χ^2, therefore a uniform correction to the centroids was applied before extracting the energies using the energy curve obtained from the prior calibration spectrum. It was assumed that the magnitude of the drift scaled proportionally with the time between counting, so the result in Fig. 3 for the two Sb spectra was normalized according to the time difference between the calibration measurement and the Sb^2 count. This resulted in a centroid correction of 0.017(27) channels.

For both Sb spectra the energy calibration was performed in the usual way by first tabulating γ-ray energy as a function of ADC channel number. A least-squares fit was performed on each peak using a symmetric Gaussian function on top of a linear background with the centroids and uncertainties determined from the fits using the γ-ray spectroscopy analysis software GAUSS [15]. Such a function provided good fits for all peaks above ~250 keV. At lower energies, it is evident

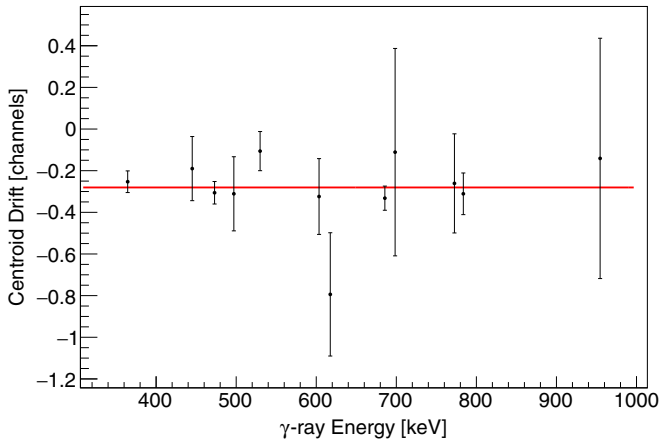

FIG. 3. The differences in centroid channels for various γ-ray lines between the two Sb sample measurements are shown as a function of energy. The red line shows the best fit to the data.

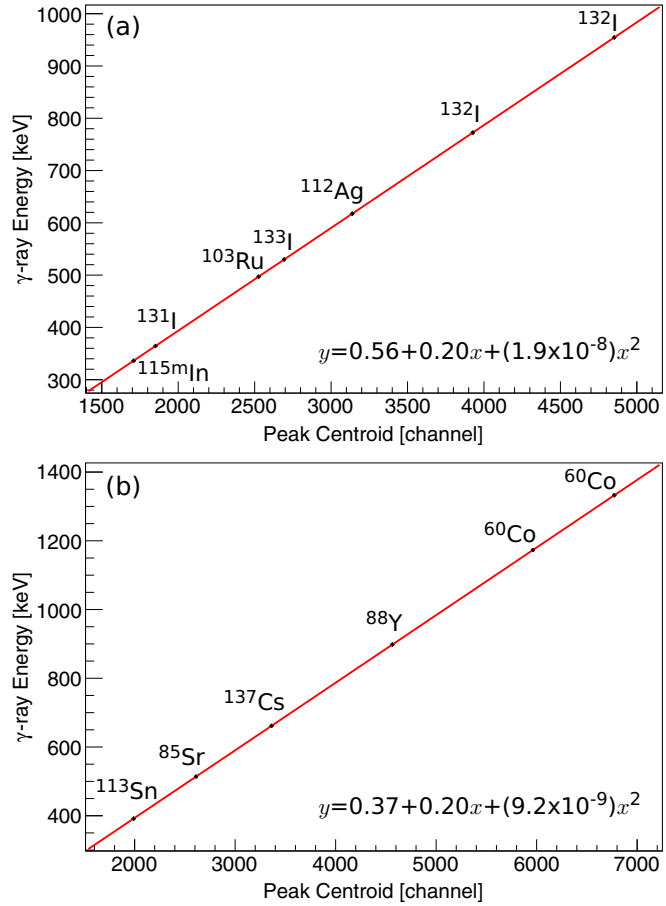

FIG. 4. The energy calibration curves obtained from (a) contaminant peaks in the Sb^1 spectrum and (b) from the calibration spectrum recorded just before the Sb^2 count. In both cases the deviations from linearity are small over the fitted channel ranges.

that a step-like component must be included in the fit function to accurately model the peak shapes, particularly those with high intensities [16] (e.g., the 140 keV ^{99m}Tc peak in Fig. 2). Furthermore, there were few quality calibration lines below 330 keV in the Sb^1 spectrum which prevented a precise energy calibration at low energies. Both calibrations were obtained by fitting the γ-ray energies against their corresponding channel centroids using a second-order polynomial (Fig. 4). No improvement in the fit for Sb^1 was obtained by increasing the polynomial order to 3, while in the calibration spectrum for Sb^2 only a marginal improvement was obtained. The latter could be an artifact of the larger fit range used for the Sb^2 calibration and/or possibly due to localized nonlinearities in the ADC [16], which was not tested during the experiment. Nevertheless, in order to account for this possibility in the overall uncertainties of the results, the deviations in energy values between the second- and third-order polynomial fit functions were included in the values reported for Sb^2. Generally speaking, the deviations were quite small, on the order of 10 eV or less, and comprised only a minor component of the overall uncertainties. Moreover, below ~350 keV, presumably for reasons related to the discussion above, the fit quality of the polynomial function (for all orders) deteriorated, so only ^{127}Sb γ-ray energies between 390 and 1300 keV are reported with new values. It is no surprise, however, that the accuracy of the fit would be reduced as a wider range of the ADC is included [16]. Luckily the majority of ^{127}Sb lines have energies that fall within this range; the most significant lines with lower energies sit at 290.8, 252.4, and 61.1 keV [11], but those values seem to be consistent with our rough energy calibration of the whole spectrum obtained using a simple linear function.

Since both spectra contain a significant number of non-^{127}Sb lines, it is important to ensure that none of the lines of interest contain interferences that would alter the final energy and intensity values. To check this, all lines with measurable areas were identified according to their emitting isotopes and all identified ^{127}Sb lines were checked against the adopted decay γ rays [12] for each found isotope to see if any known interferences with non-negligible intensities existed. Furthermore, the peak width function was obtained from the calibration spectrum (fitting with a second-order polynomial, see Fig. 5), and all peak fits were checked against that function to make sure the widths were not too large indicating possible interference. The only ^{127}Sb peak with an interference that prevented a determination of its energy and intensity was the 667.5 keV line [11], which was covered by the strong 667.7 keV line from ^{132}I.

The final results for γ-ray energies and uncertainties obtained from Sb^2 are provided in Table I. They are compared with results from Sb^1 where possible, as well as the adopted values from the evaluation of Ref. [11] for ^{127}Sb β decay (p. 1695), and also the ^{127}Te adopted γ rays (p. 1689) which were largely influenced by the (n, γ) measurement reported in Ref. [17]. It is seen that there is generally good agreement between the various data sets. To provide further validation of the present measurement, the γ-ray energies of the contaminant lines remaining in Sb^2 are compared with database values taken from Ref. [12] in Table II, showing excellent agreement. This provides added confidence in the ^{127}Sb energy values tabulated in Table I.

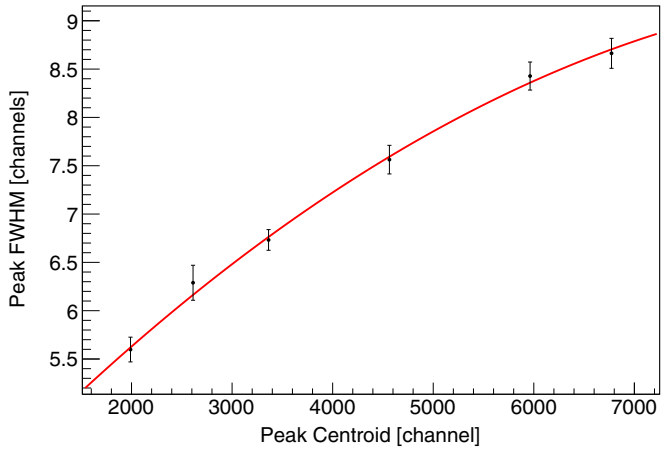

FIG. 5. The spectral width function was obtained by fitting peaks from ^{113}Sn, ^{85}Sr, ^{137}Cs, ^{88}Y, and ^{60}Co in the mixed isotope standard recorded in the calibration spectrum.

As an additional check, the ratios of peak areas for ^{127}Sb lines in the two measurements are plotted in Fig. 6 to ensure they agreed with expectations based on the known half-life of 3.85(5) d [11]. One sees from the figure that the values show reasonable agreement with the expected ratio, however there is a systematic shift towards a slightly lower value. Since the two counts were recorded only 20 h apart, small compared to the ^{127}Sb lifetime, and also limited by statistics, the measurement cannot provide any improvement of precision to the evaluated half-life. The half-life determined from the fit of measured ratios in Fig. 6 is 3.2(3) d which is 2σ from the evaluated value. The present value lacks precision for the reasons mentioned above but may also contain a systematic error caused by slightly different absolute detector efficiencies for the two counts. Indeed, based on the present

TABLE II. The measured γ-ray energies from contaminants in the Sb^2 spectrum are compared with their corresponding evaluated values. The good agreement provides validation of the Sb^2 calibration.

Parent isotope	Eval. E_γ [keV] NNDC	Meas. E_γ [keV] Sb^2
^{131}I	364.489(5)	364.426(24)
^{126}Sb	414.7(2)	414.741(37)
^{127}Te	417.9(1)	418.064(76)
^{103}Ru	497.085(10)	497.094(25)
^{133}I	529.872(3)	529.901(21)
^{112}Ag	617.517(3)	617.455(53)
^{131}I	636.989(4)	636.921(81)
^{126}Sb	697.0(4)	697.17(18)
^{126}Sb	720.7(4)	720.43(12)
^{131}I	722.911(5)	722.91(23)
^{132}I	772.60(1)	772.662(45)
^{125}Sn	822.48(5)	822.30(18)
^{132}I	954.55(9)	954.68(11)
^{125}Sn	1067.10(5)	1067.09(15)
^{132}I	1136.00(2)	1136.36(35)
^{133}I	1298.223(5)	1298.13(15)

TABLE I. The γ-ray energies obtained from the present measurements compared with the evaluated values from Refs. [11,12]. Note that the γ rays of interest are emitted by the excited daughter nucleus ^{127}Te following ^{127}Sb β decay.

Eval. $E_{\text{Lev.}}$ [keV] ^{127}Sb β decay	Eval. E_γ [keV] ^{127}Sb β decay	Meas. E_γ [keV] Sb^1 count	Meas. E_γ [keV] Sb^2 count	Eval. E_γ [keV] ^{127}Te adopted
473.24(25)	412.1(5)		412.002(23)	412.0(1)
	473.0(4)	473.187(12)	473.163(14)	473.3(1)
502.9(4)	441.0(9)		440.679(93)	440.77(2)
	502.8(6)		502.021(69)	501.93(1)
631.0(9)	543.3(5)		543.236(31)	543.2(1)
685.5(5)	685.7(5)	684.866(15)	684.899(16)	685.0(1)
783.4(3)	722.2(5)		721.48(11)	721.8(5)
	783.7(5)	782.512(23)	782.570(16)	782.63(3)
785.2(10)	445.1(5)	445.268(25)	445.257(21)	445.26(3)
	698.5(5)	697.860(65)	697.940(76)	697.9(1)
924.3(6)	451.0(7)		451.00(16)	451.0(7)
	584.2(11)		583.34(12)	583.0(4)
	924.4(9)		924.10(10)	924.0(3)
1077.0(5)	391.8(5)		391.997(44)	391.8(3)
	603.5(5)	603.796(30)	603.811(28)	604.1(2)
1140.9(5)	637.8(5)		638.21(20)	638.3(1)
	1141.6(8)		1140.23(16)	1139.90(23)
1155.4(7)	652.3(9)		652.84(13)	652.8(1)
	682.3(10)		681.56(14)	681.3(2)
1290.3(5)	817.0(6)		816.269(92)	816.6(2)
	1290.3(8)		1289.82(15)	1289.4(3)
1323.4(8)	820.6(6)		819.68(16)	820.6(6)

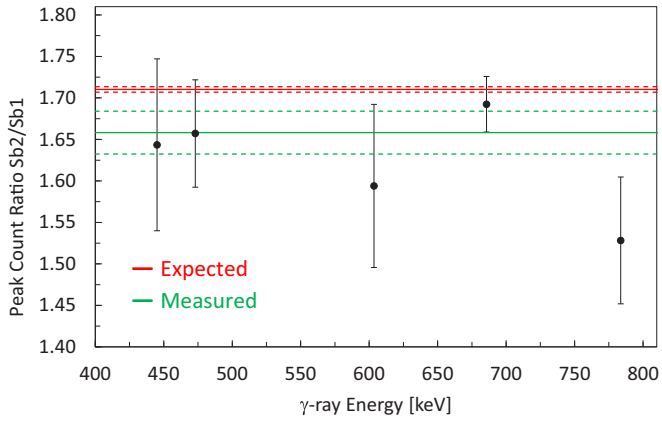

FIG. 6. The ratios of absolute counts in the strongest ^{127}Sb decay peaks between the Sb^1 and Sb^2 measurements. The red solid line shows the expected ratio based on the evaluated ^{127}Sb lifetime and the Sb^1 and Sb^2 count lengths and dates. The green solid line shows the best fit to the measured data. The dashed lines indicate 1σ standard deviations.

experimental configuration, such a shift in absolute efficiency can be accounted for by a change in source to detector distance of only 2 mm, where the precision of the distance from count to count is only considered good to within 5 mm. However, this is of no consequence to the measured relative intensities provided in Table III which require only the relative efficiency measurement provided by the curve in Fig. 1. Those values are also compared to the evaluated values of Ref. [11] and show good agreement.

IV. RESULTS

The most significant results of this measurement are the discrepancies of γ-ray energies for the first- and third-most intense lines in ^{127}Sb decay. The evaluated database values are adopted from the 1967 work of Ragaini *et al.*, based on radiochemical separations of Sn and Sb isotopes from enriched U_3O_8 targets irradiated with reactor neutrons [18]. The subsequent decay spectroscopy was done using a Ge(Li) detector whose energy resolution was limited to 2.6 keV (FWHM) for the 662 keV ^{137}Cs line. The finite detector resolution likely contributed to the large quoted uncertainties in the energies (see Table I), however a systematic error in the energy calibration near ~700 keV was apparently introduced from the use of the calibration isotope ^{54}Mn whose γ-ray line at 834.848(3) keV [12] was overestimated at the time to be 835.50(15) keV [19]. This would explain the overestimation of γ-ray energies by Ragaini *et al.* in this energy region relative to the presently reported values and those recorded from ^{126}Te(n,γ) [17] in Table I.

Despite the large absolute discrepancies of ~1 keV in energy values of these intense lines, due to the low precision of the Ragaini *et al.* measurement, these amount to only ~2σ deviations. Nevertheless, for practical applications this can be quite significant, since a discrepancy of ~1 keV in a reasonably well-calibrated γ-ray spectrum would make any such assignment highly doubtful. Typically, γ-ray energies

TABLE III. Intensities of γ-rays emitted following ^{127}Sb β decay relative to the strong 685 keV line. The evaluated values are taken from Ref. [11]. Lines in *italic* were not observed in the present experiment, but are listed in the evaluation. For completeness, upper limits on their intensities have been provided, which are consistent with the evaluated values.

Eval. E_γ [keV]	Eval. rel. int.	Meas. rel. int. (Sb^2)
61.1	3.9(3)	6.01(82)
154.3	*0.4(2)*	*<1.20*
252.4	23.1(9)	21.27(97)
280.4	1.8(4)	1.00(18)
290.8	5.5(3)	4.54(31)
293.3	0.8(4)	0.44(17)
310.0	0.7(3)	1.03(24)
391.8	2.6(2)	2.94(25)
412.1	10.4(11)	9.76(51)
441.0	1.9(9)	1.35(22)
445.1	11.8(3)	11.50(58)
451.0	0.5(2)	0.78(21)
456	*0.3(2)*	*<1.10*
473.0	70.1(19)	67.6(27)
502.8	2.1(7)	2.56(34)
543.3	8.0(12)	8.45(51)
584.2	0.9(5)	0.23(7)
603.5	12.1(3)	12.25(66)
624	*0.18(6)*	*<1.47*
637.8	1.2(4)	1.48(43)
652.3	1.0(2)	1.00(25)
667.5	2.0(2)	<3.3
682.3	1.5(7)	0.90(20)
685.7	100	100
698.5	9.9(2)	8.1(13)
722.2	5.1(3)	4.44(61)
745.9	*0.4(2)*	*<0.97*
763.7	*0.2(1)*	*<0.89*
783.7	41.1(9)	40.4(18)
817.0	1.1(5)	1.23(22)
820.6	0.6(3)	0.52(15)
924.4	1.4(2)	1.55(23)
1141.6	1.0(2)	1.23(22)
1155.2	*0.11(6)*	*<0.81*
1290.3	1.0(3)	0.96(19)
1377.9	*0.2(1)*	*<0.65*

from isotopes with decay lifetimes on the order of days or longer are much more precisely measured and such is generally assumed in the analysis of complicated spectra like those produced from fission. The analysis of spectra for nuclear forensic applications is particularly vulnerable since they can involve a complicated array of activation products as well as a dynamic set of fission products that are simultaneously decaying away and growing in depending on the amount of time elapsed between the event in question and the measurement. Therefore, it is extremely important to have as accurate (and precise) nuclear data as possible to facilitate an easier and more reliable analysis of γ-ray spectra. The ^{127}Sb fission product could be a particularly important example because of its optimal lifetime for forensic analysis,

its decay strength concentration in only a few γ-ray lines having energies above the busiest spectral region where the Compton background and density of photopeaks are highest, and its relatively high but distinct cumulative yields from the various common fission mechanisms; i.e. ^{235}U thermal neutron-induced, ^{238}U fast neutron, ^{239}Pu thermal, etc. [9,10].

V. CONCLUSIONS

New measurements of ^{127}Sb β decay have been performed based on radiochemical separations of various fission products produced from photofission of uranium. Following careful energy and efficiency calibrations of a HPGe detector over a limited signal range, a new, more precise set of characteristic γ-ray energies and associated intensities have been obtained. The most significant results are the energy shifts observed for the first- and third-most intense decay lines which are on the order of 1 keV. This has important implications on forensic analysis of fallout debris that could be collected shortly following a nuclear event, as such large errors in evaluated nuclear data complicate and inhibit an accurate isotopic analysis. This result highlights the importance of continued experimental efforts aimed towards key nuclear data, even for cases (like ^{127}Sb β decay) where the lifetimes are significantly long and experimental data dates back several decades.

ACKNOWLEDGMENTS

The authors gratefully acknowledge the support of J. Stoner, J. Longley, and the staff at the Idaho Accelerator Center as well as R. Watson, R. Farrar, and their staff at INL's Analytical Laboratory. This material is based upon work supported in part by DTRA under IAA HDTRA1618618. This manuscript has been authored by Battelle Energy Alliance, LLC under Contract No. DE-AC07-05ID14517 with the U.S. Department of Energy.

[1] R. Stone, Science **351**, 1138 (2016).
[2] K. J. Moody, P. M. Grant, and I. D. Hutcheon, *Nuclear Forensic Analysis* (CRC Press, Boca Raton, FL, 2015).
[3] K. P. Carney, M. R. Finck, C. A. McGrath, L. R. Martin, and R. R. Lewis, J. Radioanal. Nucl. Chem. **299**, 363 (2014).
[4] F. L. Lisman, W. J. Maeck, and J. E. Rein, Nucl. Sci. Eng. **42**, 215 (1970).
[5] T. Straume, G. Rugel, A. A. Marchetti, W. Rühm, G. Korschinek, J. E. McAninch, K. Carroll, S. Egbert, T. Faestermann, K. Knle, R. Martinell, A. Wallner, and C. Wallner, Nature (London) **424**, 539 (2003).
[6] E. M. Burbidge, G. R. Burbidge, W. A. Fowler, and F. Hoyle, Rev. Mod. Phys. **29**, 547 (1957).
[7] E. C. Freiling, Science **133**, 1991 (1961).
[8] Y. A. Izrael, *Radioactive Fallout After Nuclear Explosions and Accidents* (Elsevier Science, Oxford, 2002).
[9] T. R. England and B. F. Rider, Evaluation and Compilation of Fission Product Yields, ENDF-349, LA-UR-94-3106 (Los Alamos National Laboratory, 1994).
[10] M. Mac Innes, M. B. Chadwick, and T. Kawano, Nucl. Data Sheets **112**, 3135 (2011).
[11] A. Hashizume, Nucl. Data Sheets **112**, 1647 (2011).
[12] Brookhaven National Laboratory, NNDC Nuclear Database, http://www.nndc.bnl.gov/ (accessed June 2018).
[13] http://www.iac.isu.edu.
[14] Eckert & Ziegler Isotope Products, Eckert & Ziegler Reference & Calibration Sources, https://www.ezag.com/fileadmin/user_upload/isotopes/isotopes/Isotrak/isotrak-pdf/Product_literature/EZIPL/EZIP_catalogue_reference_and_calibration_sources.pdf (accessed August 2018).
[15] R. G. Helmer and C. M. McCullagh, Nucl. Instrum. Methods **206**, 477 (1983); A. J. Caffrey, A. E. Egger, and B. C. Hadden, *Gauss XI User's Manual*, *INL/EXT-11-24120-REV1* (Idaho National Laboratory, 2013).
[16] K. Debertin and R. G. Helmer, *Gamma- and X-Ray Spectrometry with Semiconductor Detectors* (Elsevier Science B. V., Amsterdam, The Netherlands, 1988).
[17] J. Honzátko, V. Bondarenko, I. Tomandl, T. von Egidy, H.-F. Wirth, D. Bucurescu, V. Ponomarev, N. Mărginean, R. Hertenberger, Y. Eisermann, G. Graw, and L. Rubáček, Nucl. Phys. A **756**, 249 (2005).
[18] R. C. Ragaini, G. E. Gordon, and W. B. Walters, Nucl. Phys. A **99**, 547 (1967).
[19] G. Graeffe, C. W. Tang, C. D. Coryell, and G. E. Gordon, Phys. Rev. **149**, 884 (1966).